Simulated "Air Bleed" Oxidation of Adsorbed CO on Carbon Supported Pt. Part 2. Electrochemical Measurements of Hydrogen Peroxide Formation during O_2 Reduction in a Double-Disk Electrode Dual Thin-Layer Flow Cell

Z. Jusys and R. J. Behm*

Department of Surface Chemistry and Catalysis, University Ulm, D-89069 Ulm, Germany

Received: January 7, 2004; In Final Form: April 1, 2004

The reaction of preadsorbed CO with O_2 and the simultaneous O_2 reduction reaction (ORR) on a carbon supported Pt catalyst (20%Pt/Vulcan) in an O_2-saturated electrolyte at potentials of 0.06 V and, for comparison, at 0.26 V_{RHE} were investigated by electrochemical measurements in a dual thin-layer flow cell under continuous flow conditions. Following a previous differential electrochemical mass spectrometry study (*J. Electroanal. Chem.* **2003**, *554*−*555*, 427), which demonstrated very slow CO_2 formation, in combination with significant O_2 consumption, even at the most cathodic potential (0.06 V_{RHE}), we here show that the O_2 consumption on the CO_{ad}-saturated catalyst is due to almost exclusive H_2O_2 formation. Both the CO oxidation rate and the selectivity for H_2O_2 formation decrease with lower CO_{ad} coverage, reaching slightly above 25% at the limiting coverage of 80% of the saturation value (0.6 monolayers). The experimental observations are explained by a mechanism, where H_2O_2 formation and, with a much lower probability, reaction with a neighboring CO_{ad} occur upon O_2 adsorption in monomer vacancies. For O_2 adsorption on larger vacancy islands dissociative adsorption and subsequent H_2O formation prevails, reaction with CO_{ad} at the perimeter of the vacancy island is practically inhibited. Consequences for the air bleed operation of polymer electrolyte fuel cells are discussed.

1. Introduction

The "air bleed" reaction,[1] the reaction of adsorbed CO on the anode catalyst with small amounts of O_2 added to the feed gas, was proposed as a simple and inexpensive method to reduce the poisoning of the anode catalysts (carbon supported Pt or Pt alloy catalysts) by adsorbed CO in low-temperature polymer electrolyte membrane fuel cells (PEFCs), which are operated by CO-contaminated H_2-rich gases produced by reforming of hydrocarbons and methanol (ref 2 and references in ref 3). Inspite of its technical importance, however, this reaction has rarely been studied, and details of the reaction mechanism and kinetics of this process are largely unknown (see also ref 3). In this context, it is important to note that under PEFC anode operation conditions, at potentials around 0.05−0.1 V_{RHE}, both oxygen reduction and hydrogen peroxide formation can occur at the fuel cell anode, when O_2 is present in the anode feed, either from direct O_2 admission via the feed gas (air bleed) and/or due to possible O_2 crossover through the ionomer membrane from the cathode side.[4] Formation of hydrogen peroxide at the membrane electrode assembly (MEA) is highly undesirable, since it will cause increased degradation of both the gas diffusion layer and the ionomer membrane under fuel cell operating conditions.[5,6]

We have therefore started to systematically investigate the reactions accompanying the air bleed operation in more detail. In a preceding paper,[3] we reported results of an on-line mass spectrometric study of a simulated air bleed reaction on a Pt/Vulcan catalyst, monitoring on-line both CO_2 formation and O_2 consumption on the CO_{ad}-covered catalyst as a function of the electrode potential and reaction time by differential electrochemical mass spectrometry (DEMS). In that study, we found a significant depletion of O_2 in the electrolyte in the potential region of hydrogen underpotential deposition (H-upd) on the CO_{ad}-blocked surface, which was tentatively attributed to hydrogen peroxide formation. Continuing that study, we now directly investigated and determined the hydrogen peroxide yields on CO_{ad}-blocked Pt/Vulcan catalyst electrodes in O_2-saturated solution by using a dual disk-electrode dual thin-layer flow cell (DDE- DTLFC). The design of the setup is described in more detail and characterized in ref 7. The results of these measurements, which show an extremely high current efficiency of up to nearly 100% for hydrogen peroxide formation on a CO-blocked Pt/Vulcan catalyst in the H-upd region, are reported and discussed in the present paper.

The formation of hydrogen peroxide during the oxygen reduction reaction (ORR) on Pt surfaces and catalysts at fuel cell relevant potentials in the range of 0.05−0.1 V_{RHE} is well documented and has been widely studied using the rotating ring-disk electrode (RRDE) technique (for polycrystalline Pt see, e.g., refs 8−10, for single-crystal Pt(*hkl*) electrodes see refs 11−13, and for supported Pt catalysts see refs 14−20). O_2 reduction to water (four-electron process), which is the dominant process on Pt electrodes/catalysts at potentials $>0.3V_{RHE}$ (see above references), is known to be hindered by adsorbed species,[21,22] such as adsorbed (bi)sulfate, chloride or bromide anions,[18,23,24] adsorbed selenium or sulfur,[25] or adsorbed hydrogen, upon H-upd.[11] Similar effects have been reported for Pt surfaces modified by oxide formation (OH adsorption)[26] or by Cu-upd deposition.[27,28] On the other hand, rotating ring disk electrode (RRDE) measurements showed a significant increase of hydrogen peroxide production on the adsorbate blocked surfaces compared to the clean Pt surfaces.[11,18,21,23−28] This change in reaction pathway, from a four-electron pathway to a two-electron

* To whom correspondence should be addressed. E-mail: juergen.behm@chemie.uni-ulm.de.

10.1021/jp0499171 CCC: $27.50
Published on Web 05/12/2004

pathway, was attributed to a blocking of surface sites on the Pt surface required for the dissociative adsorption of O_2.

In the present situation, where we are interested in hydrogen peroxide formation on a CO_{ad}-covered surface in O_2-containing electrolyte at potentials typical for PEFC anodes (0.05−0.1 V_{RHE}), the commonly used RRDE approach is hardly applicable because of experimental problems, due to the relatively long time required for electrolyte exchange (or saturation by O_2) and the immediate onset of CO_{ad} oxidation upon contact with the oxygen-containing electrolyte. Hence, in an RRDE setup, CO oxidation would start already before saturation of the electrolyte.[21] This is different in a flow cell, and our DDE-DTLFC design allows a fast change of electrolyte, from a CO-saturated electrolyte to an O_2-containing electrolyte, under well controlled conditions (for details see ref 7).

After a brief description of the experimental setup and details, we will present and discuss the results of potentiodynamic and transient potentiostatic measurements on the ORR kinetics and on the CO adlayer oxidation in O_2-saturated solution CO_{ad}-covered Pt/Vulcan electrodes. For comparison, we include also measurements on CO_{ad}-free Pt/Vulcan electrodes and on Pt-free carbon Vulcan electrodes. The resulting data will demonstrate that under fuel cell relevant conditions on a fully or largely CO_{ad}-covered Pt/Vulcan electrode the majority of the consumed O_2 will be reacted into H_2O_2 rather than being used for CO oxidation.

2. Experimental Section

The experimental setup for the dual disk electrode thin-layer flow cell measurements was described and characterized in detail in a previous publication.[7] In short, it is based on the dual thin-layer flow cell design described in ref 29, which had been used for DEMS measurements on supported catalyst electrodes in our group (see ref 3 and references therein) and which was modified for the present measurements. The cell itself cell consists of a circular Kel-F plate (5 mm thick) with capillaries for the electrolyte inlet and outlet, whose openings are located at the center of the Kel-F plate, on the opposite sides, and two electrodes which are pressed via two sealing gaskets (Kalrez, ca. 50 μm thick) against the Kel-F plate. The working electrode in the first compartment (generator) is a mirror-polished glassy carbon disk 9 mm in diameter covered with a thin Pt/Vulcan or Vulcan carbon film (6 mm diameter), and the collector electrode is a mirror-polished polycrystalline Pt disk (15 mm in diameter, exposed area 1.33 cm^2).

The thin-film electrode was prepared as described previously,[30] by pipetting an aliquot of an aqueous suspension of the Pt/Vulcan catalyst (E-TEK, 20 w.% Pt) onto the glassy carbon disk (Sigradur G, from Hochtemperatur Werkstoffe) and then a defined amount of Nafion solution on top of the dried catalyst layer. The latter results in a very thin (ca. 0.1 μm thickness) Nafion film. The geometric area of the accessible part of the electrode is 0.28 cm^2, the Pt loading 28 $\mu g\ cm^{-2}$. The average particle size and the particle size distribution of the Pt/Vulcan catalyst had been characterized recently by X-ray diffraction (XRD) and transmission electron microscopy (TEM), yielding an average particle size of 3.7 nm for the conditioned catalyst and a dispersion of 26%.[31] Prior to the calibration and kinetic measurements, both electrodes were characterized by cyclic voltammetry (CV) in 0.5 M H_2SO_4 solution.[7]

Two Pt wires connected through separate ports at the inlet and outlet of the cell served as counter electrodes. The reference electrode, a saturated calomel electrode (SCE), was connected trough a Teflon capillary at the outlet of the cell. (All potentials are quoted, however, vs that of the reversible hydrogen electrode (RHE)). The electrolyte flow (flow rate ca. 4 μL/s) was driven by the hydrostatic pressure of the electrolyte in the supply bottle, which was continuously purged by Ar or saturated with O_2. Under these flow conditions electroactive species formed at the generator electrode were detected at the potential-controlled collector electrode with a delay of ca. 3 s and a collection efficiency of 76% (for details of the calibration see ref 7).

The supporting electrolyte (0.5 M sulfuric acid) was prepared using Millipore Milli Q water and ultrapure sulfuric acid (Merck, suprapur) and purged by high purity Ar (MTI Gase, N 6.0) or saturated with O_2 (MTI Gase, N 5.7) in the electrolyte supply bottle. For the chronoamperometric and CO stripping experiments, CO was preadsorbed at a constant electrode potential for 10 min, after introducing 2 mL of 0.5 M H_2SO_4 solution saturated with CO (Messer-Griesheim, N 4.7) by an all-glass syringe through a separate port. Then the cell was rinsed by introducing Ar-saturated solution through the same port, using another syringe. Finally, the O_2-saturated electrolyte was admitted to the cell by opening an open-close valve at the electrolyte supply bottle. CO_{ad} stripping experiments were performed either immediately after having started the flow of O_2-saturated electrolyte or at the end of a chronoamperometric measurement in the same electrolyte. In both cases, CO stripping was performed in O_2-saturated electrolyte. The CO stripping measurements were followed by a second complete potential cycle, detecting the O_2 reduction behavior on a CO-free electrode. By comparison with previous data (see ref 7 and references therein), the latter measurements can also be used to check the cleanness of the electrode. All measurements were conducted at room temperature.

3. Results

3.1. Oxygen Reduction on Pt/Vulcan Catalyst Electrodes − Potentiodynamic Measurements. *3.1.1. Oxygen Reduction on CO_{ad}-Saturated Pt/Vulcan Catalysts.* The oxidation of the CO adlayer and the O_2 reduction behavior in the O_2-saturated electrolyte on CO_{ad}-precovered Pt/Vulcan electrodes were first investigated in potentiodynamic DDE-DTLFC experiments, starting with a Pt/Vulcan catalyst saturated with preadsorbed CO_{ad} at 0.06 V. The combined oxygen reduction and CO oxidation current on the Pt/Vulcan generator electrode and the hydrogen peroxide oxidation current on the polycrystalline Pt collector electrode at 1.16 V were detected simultaneously. The resulting cyclic voltammetry DDE-DTLFC data for the ORR are shown in Figure 1. The solid black line in Figure 1a (total Faradaic current $I_{F(total)}$) represents the first positive-going scan, recorded immediately after starting the flow of O_2-saturated 0.5 M H_2SO_4 solution through the DDE-DTLFC cell. The gray solid line in Figure 1a describes a subsequent CV of the Pt/Vulcan electrode in O_2-saturated solution, corresponding to the ORR in O_2-saturated base electrolyte on the unmodified Pt/Vulcan catalyst electrode. This CV is basically identical with previous DDE-DTLFC data published in ref 7, underlining both the cleanness of the electrode and the reproducibility of the measurements.

The measured Faradaic current ($I_{F(total)}$) response to the electrode potential scan shows a complicated behavior: Immediately after starting the electrolyte flow (still at 0.06 V), the current on the CO_{ad}-covered Pt/Vulcan electrode increases to ca. −0.15 mA, which is about $^1/_3$ of the mass transport limited ORR current in the subsequent scan. When the potential is increased, the current first diminishes to ca. −0.8 mA at about 0.15 V and then increases again, approaching nearly the mass

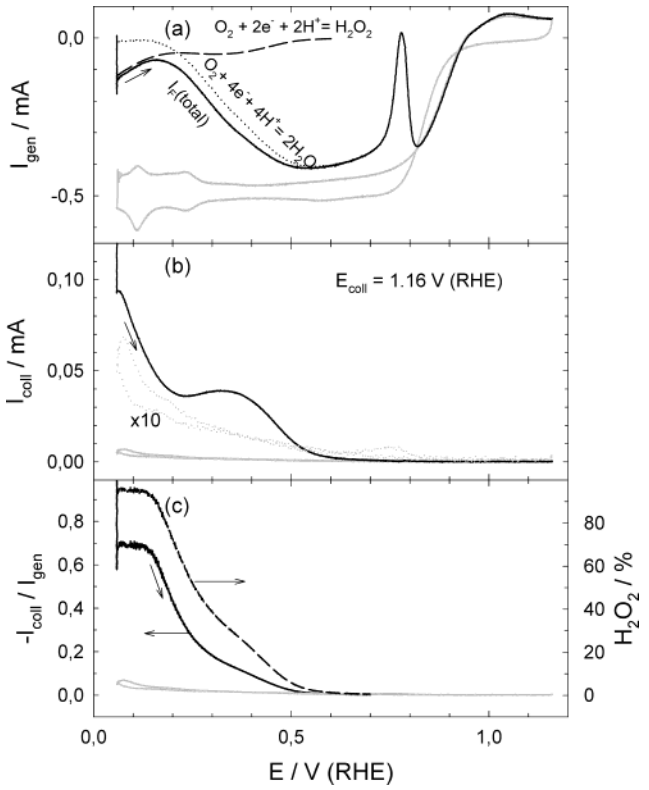

Figure 1. Simultaneously recorded cyclic voltammogram on a CO_{ad}-blocked Pt/Vulcan catalyst (Pt loading 28 μg/cm^2, CO preadsorption at 0.06V) in the first compartment of a dual thin-layer flow cell in O_2-saturated 0.5 M H_2SO_4 solution (a), simultaneously measured H_2O_2 oxidation current measured on a polycrystalline Pt electrode ($E = 1.16$ V) in the second compartment (b), and hydrogen peroxide yield (c). Electrolyte flow rate ca. 4 μL/s, potential scan rate 10 mV/s, room temperature. Black solid lines correspond to the first positive-going scan. Solid gray lines correspond to subsequent cyclic voltammogram in a supporting electrolyte. Dotted gray line in (b): similar to the solid gray line, but enhanced sensitivity ($\times$10). Dashed black line (a): partial current for oxygen reduction to hydrogen peroxide calculated according to eq 1. Dotted black line (a): partial current for oxygen reduction to water calculated as the difference between the net current and partial hydrogen peroxide formation current.

transport limited oxygen reduction current in the potential region between 0.5 and 0.7 V (ca. -0.4 mA). This is followed by the characteristic CO_{ad} electrooxidation peak centered at ca. 0.77 V, and finally, the current signal traces the behavior of a Pt/Vulcan catalyst in an O_2-saturated solution at potentials positive of 0.82 V (Figure 1a, solid gray line). The complex character of the current response results from several contributions, namely oxygen reduction (both to hydrogen peroxide and water), adsorbed CO oxidation (both electrochemical and chemical oxidation), which may contribute directly (electrochemical oxidation) and indirectly via a CO_{ad}-coverage dependent ORR rate, and the voltammetric features of the Pt/Vulcan electrode itself.

Information on the amount of CO oxidation and on the evolution of the CO_{ad} coverage during the CV comes from previous DEMS measurements of the same reaction and on the same catalyst,[3,32] which had shown that the increase in Faradaic current during the positive-going scan goes along with the oxidation of $\sim$0.05 ML of CO_{ad} in the potential range 0.06$-$0.4 V, and additional $\sim$0.15 ML (0.2 ML in total) at the onset of the main CO stripping peak.

The formation of hydrogen peroxide during reaction of the CO presaturated Pt/Vulcan electrode in the O_2 saturated solution was monitored via the collector current (Figure 1b, solid black line). At 0.06 V, the hydrogen peroxide formation rate on the CO_{ad}-covered Pt/Vulcan surface is more than 1 order of magnitude higher than on the CO-free catalyst surface as measured in the second scan (Figure 1b, solid gray line). For better visualization, the latter is included also on a 10-fold magnified scale (Figure 1b, dotted gray line). The difference is even more pronounced, by a factor of 20, in the double-layer region, between 0.3 and 0.6 V. The ratio between the collector current (corrected by the time constant of the setup) and the generator current is about constant at ca. 0.76 in the potential range 0.06$-$0.15 V (Figure 1c, solid black line). Depending on the potential, it is 1$-$2 orders of magnitude higher than on the CO-free Pt/Vulcan catalyst in the potential range up to 0.6 V (Figure 1c, gray line). Taking into account the collection efficiency of our DDE-DTLFC setup of 76%,[7] the current efficiency for hydrogen peroxide formation reaches about 90% on the CO_{ad}-saturated Pt/Vulcan surface at potentials negative of 0.15 V (Figure 1c, dashed line). Similarly high current efficiencies for hydrogen peroxide production during the ORR of up to 100% have been reported in several RRDE studies on adsorbate-covered Pt electrodes, e.g., on selenium-modified polycrystalline Pt in the range of Se-adlayer stability,[25] on adsorbed bromide-covered Pt(111) in the double-layer region (0.2$-$0.4 V),[23] and on H_{ad}-covered Pt(111) in the H$-$UPD region,[11] i.e., on Pt surfaces which were blocked by adsorbed species under reaction conditions. In a recent RRDE measurement of the ORR on a CO_{ad}-blocked Pt/Vulcan catalyst,[21] the initial H_2O_2 yield was much lower, about 10%, but increased to a similar value of about 80%. This discrepancy is tentatively attributed to the undefined, low O_2 concentration in the electrolyte at the beginning of that experiment.

The two partial currents $I_{H_2O_2}$ and I_{H_2O}, which were calculated from the time constant-corrected collector current I_{coll} via the relations

$$I_{H_2O_2} = I_{coll}/N \tag{1}$$

where N represents the collection efficiency ($N = 0.76$) and

$$I_{H_2O} = I_{gen} - I_{H_2O_2} = I_{gen} - I_{coll}/N \tag{2}$$

are plotted as a dashed black line ($I_{H_2O_2}$) and dotted black line (I_{H_2O}), respectively, in Figure 1a as a function of the electrode potential, up to the onset of adsorbed CO electrooxidation. (At higher potentials, this method can no longer be applied due to increasing contributions of CO_{ad} stripping as a third electrochemical process). The fraction of O_2 being reduced to hydrogen peroxide, $X_{H_2O_2}$, can be calculated from the partial currents via

$$X_{H_2O_2} = 2I_{H_2O_2}/(2I_{H_2O_2} + I_{H_2O}) \tag{3}$$

At potentials negative of 0.15 V, the Faradaic current corresponds nearly quantitatively to the partial current for O_2 reduction to hydrogen peroxide, at essentially zero current for oxygen reduction to water, indicating practically 100% current efficiency for the former reaction pathway under these conditions (Figure 1c, dashed black line). Going to more positive potentials, the partial current for hydrogen peroxide formation reaches a plateau at ca. -0.05 mA in the potential region 0.2 to 0.4 V, and then drops to zero at potentials between 0.4 and 0.6 V (Figure 1a, dashed black line). At the same time, the partial current for oxygen reduction to water increases about linearly with potential, starting from ca. 0.15 to ca. 0.5 V (Figure 1a, dotted black line). These results suggest a strong potential dependence of the ORR on the CO_{ad}-covered Pt surface. A

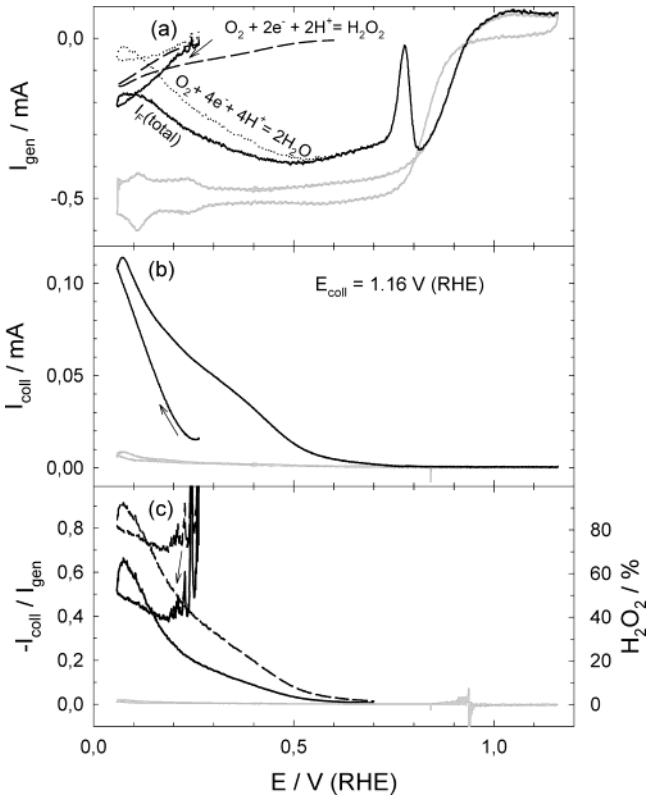

Figure 2. Simultaneously recorded cyclic voltammogram on a CO_{ad}-blocked Pt/Vulcan catalyst (E_{ad} = 0.26 V) (a), H_2O_2 oxidation current (b), and a hydrogen peroxide yield (c) in O_2-saturated 0.5 M H_2SO_4 solution, starting with a negative going scan at 0,0.26 V. (Experimental conditions and setup as well as assignment of the lines as in Figure 1.)

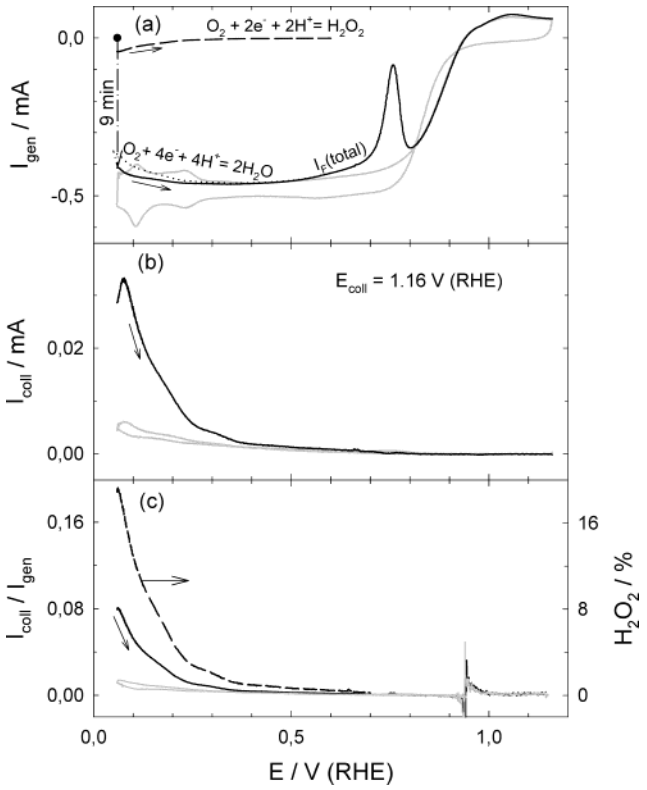

Figure 3. Simultaneously recorded cyclic voltammogram on a CO_{ad}-blocked Pt/Vulcan catalyst (E_{ad} = 0.26 V) (a), H_2O_2 oxidation current (b), and a hydrogen peroxide yield (c) in O_2-saturated 0.5 M H_2SO_4 solution, after exposure for 9 min to O_2-saturated 0.5 M H_2SO_4 solution at 0.06 V. (Experimental conditions and setup as well as assignment of the lines as in Figure 1.)

possible decrease of the CO_{ad} coverage as a result of a chemical reaction of the CO adlayer with O_2 during the positive-going potential scan cannot be ruled out, however, as origin for the decreasing H_2O_2 yield (see below). Finally, for comparison, we also include the hydrogen peroxide yield on the CO_{ad}-free Pt/ electrode determined in the second potential cycle (Figure 1c, gray line). On the scale in this graph, the hydrogen peroxide yield is hardly detectable. The maximum hydrogen peroxide yield obtained at 0.06 V is about 4%, which agrees very well with previous RRDE data.[7,17]

To clarify the question of whether the decrease in hydrogen peroxide yield with increasing potential is due to a potential effect or results from a decrease of CO_{ad} coverage, we performed an analogous ORR cyclic voltammetry experiment, where the Pt/Vulcan electrode was saturated with CO at 0.26 V and where the potential scan was started in the negative-going potential scan, immediately after having started the flow of O_2-saturated electrolyte (Figure 2). The measured (negative) Faradaic current (Figure 2a, solid black line) first increases to ca. −0.2 mA in the negative-going scan, followed by a further increases to ca. −0.4 mA at about 0.5 V during the positive-going scan. It then transforms into the peak for CO_{ad} electrooxidation, which is centered at ca. 0.77 V. At more positive potentials the signal traces the current response on the CO_{ad}-free Pt/Vulcan electrode, which was determined in the subsequent scan (Figure 2a, gray solid line). The simultaneous measurement of the collector current (Figure 2b, solid black line) shows hydrogen peroxide formation on the CO_{ad}-blocked Pt/Vulcan surface already at 0.26 V, at a rate that is about two times higher than that reached on the CO_{ad}-free Pt/Vulcan catalyst in the second cycle at the negative potential limit (Figure 2b, gray line). Hence, hydrogen peroxide formation *increases* during the negative-going potential scan up to values which are about 1 order of magnitude higher than those obtained on a CO_{ad}-free catalyst surface. In the subsequent positive-going scan, it decreases again, but remains significantly higher than in the negative-going scan and is about 20 times higher than on the CO_{ad}-free electrode over the entire potential region up to ca. 0.7 V. The ratio of the (time constant corrected) collector current to generator current (Figure 2c, solid black line) on the CO-blocked electrode surface reaches a value of ca. 0.7 at the negative potential limit, which corresponds to a hydrogen peroxide yield of ca. 95% (Figure 2c, dashed black line). Finally, the partial currents for oxygen reduction to hydrogen peroxide (Figure 2a, dashed black line) and water (Figure 2a, dotted black line), calculated following the procedure described above, show a clear potential dependence for hydrogen peroxide formation in the H-upd region on the CO_{ad}-blocked catalyst. This confirms the conclusions drawn from DEMS experiments in refs 3 and 32, where a loss of CO_{ad} was ruled out as the origin for the decay of the H_2O_2 yield during the positive-going scan, and instead potential effects were favored.

3.1.2. Oxygen Reduction on Partly CO_{ad}-Covered Pt/Vulcan Electrodes after Reaction with O_2. To test for possible effects of CO_{ad} losses on the interaction with O_2-containing electrolyte, we recorded CVs after having exposed the CO_{ad}-saturated Pt/ Vulcan electrode to an O_2-saturated solution for 9 min at two different potentials, 0.06 and 0.26 V. The resulting CVs are plotted in Figures 3 and 4, respectively. The corresponding current transients recorded during these 9 min reaction time are reproduced in Figures 5 and 6 and will be discussed later in section 3.2. Again the second CV is included as well, reflecting

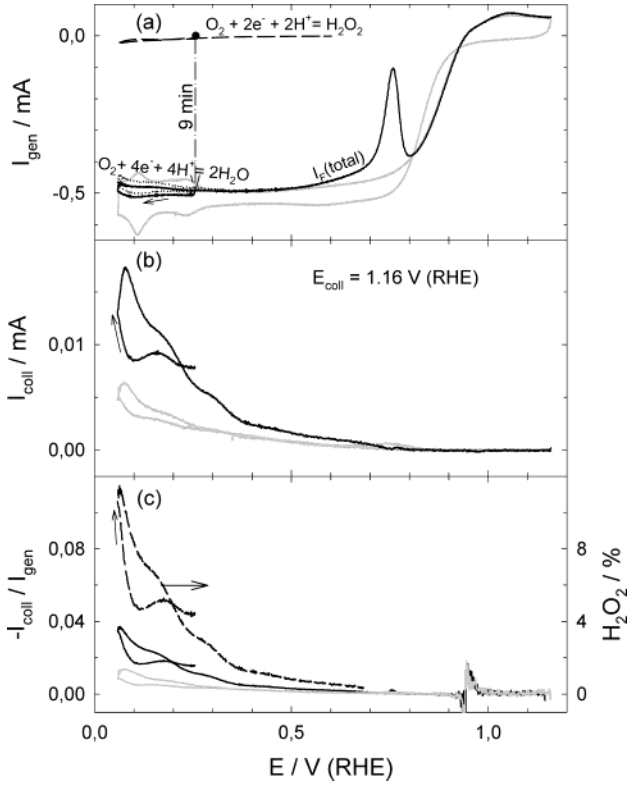

Figure 4. Simultaneously recorded cyclic voltammogram on a CO_{ad}-blocked Pt/Vulcan catalyst (E_{ad} = 0.26 V) (a), H_2O_2 oxidation current (b), and a hydrogen peroxide yield (c) in O_2-saturated 0.5 M H_2SO_4 solution, after exposure for 9 min to O_2-saturated 0.5 M H_2SO_4 solution at 0.26 V. (Experimental conditions and setup as well as assignment of the lines as in Figure 1.)

the O_2 reduction behavior on a CO_{ad}-free Pt/Vulcan electrode (Figure 3, solid gray line).

Comparison of the CV in Figure 1a, where the positive-going scan was started immediately after admitting the O_2-saturated electrolyte flow to the CO_{ad}-saturated Pt/Vulcan electrode, and that in Figure 3a, where the positive-going scan was started after the CO_{ad}-saturated Pt/Vulcan electrode was exposed for 9 min to a continuous flow of the O_2-saturated electrolyte at 0.06 V, shows that during these 9 min waiting time at 0.06 V the total ORR current has increased from about −0.15 to −0.4 mA, which is close to the mass transport limited current of −0.5 mA. (The latter current value is reached during the positive-going scan at potentials above the H-upd region, at >0.3 V (Figure 3a, solid black line).) The increase in ORR current indicates a partial loss of the blocking CO-adlayer due to chemical oxidation by reaction with oxygen during the waiting time. At more positive potentials, the characteristic CO_{ad} stripping peak appears in the positive-going scan (Figure 3a, black solid line). By subtracting the ORR current in the second positive-going scan (Figure 3a, gray solid line) and integrating the CO_{ad} stripping current in the potential range from 0.45 to 0.8 V, the charge under this peak was determined to be 1.84 mC. This is about 80% of the charge resulting from electrooxidation of a saturated CO adlayer at the same Pt/Vulcan loading (about 2.3 mC, equivalent to 0.75 monolayer (ML)[3,33]), indicative of an absolute coverage of about 0.6 ML at the end of the chemical oxidation experiment. Hence, the CO_{ad} coverage has decreased during the waiting time due to chemical oxidation in the O_2-saturated electrolyte at 0.06 V. Most of the CO_{ad} oxidation actually occurs during the first 1−2 min, which is indicated both by the initially faster increase of the Faradaic current, note that the decrease in CO_{ad} coverage is steeper than the Faradaic current increase because of the decreasing H_2O_2 yield with decreasing CO_{ad} coverage (see below), and, more directly, by the immediate CO_2 formation right above 0.06 V observed in similar potentiodynamic DEMS experiments on the same catalyst.[32]

Simultaneous measurements of the hydrogen peroxide oxidation current on the collector (Figure 3b, solid black line) show a ca. 5-fold increase compared to the value measured on the CO_{ad}-free Pt/Vulcan electrode (Figure 3b, solid gray line). Compared to the immediate positive-going scan on the CO_{ad}-saturated Pt/Vulcan electrode (Figure 1b, solid black line), however, the initial hydrogen peroxide oxidation current is reduced to about $^1/_5$. The hydrogen peroxide oxidation current corresponds to a maximum yield for hydrogen peroxide formation of ca. 18% during the ORR on the partly (ca. 20%) oxidized CO-adlayer (Figure 3c, dashed line), compared to about 95% on the fully CO_{ad}-saturated Pt/Vulcan electrode (Figure 1c, dashed line). Correspondingly, the time constant corrected partial current for oxygen reduction to hydrogen peroxide after 9 min exposure to O_2-saturated solution (Figure 3a, dashed line) is only about $^1/_5$ of that in the immediate positive-going scan (Figure 1a, dashed line), whereas the partial current for oxygen reduction to water on the partly CO_{ad}-covered electrode is close to the mass transport limited current (Figure 3a, dotted line), compared to negligible currents on a Pt/Vulcan electrode blocked by a full CO_{ad} monolayer (Figure 1a, dotted line). Hence, the ORR pathways are highly sensitive to relatively small changes in the CO_{ad} coverage, changing from nearly quantitative hydrogen peroxide formation on a Pt/Vulcan electrode blocked by a saturated CO adlayer, to about 18% hydrogen peroxide formation when about $^1/_5$ of the CO-adlayer is removed by reaction with oxygen.

Analogous cyclic voltammetry experiments were performed on the CO_{ad}-covered Pt/Vulcan surface after CO_{ad}-saturation and subsequent reaction (9 min reaction time) with O_2-saturated electrolyte at 0.26 V (Figure 4). Similarly to the results shown in Figure 3a, the ORR current reaches almost the mass transport limiting current within 9 min reaction time (the corresponding transients are shown in Figure 6). Scanning the potential first to more negative potentials, to 0.06 V, and then returning to a positive-going scan, we find that the H-upd features are still largely suppressed. Also, the pronounced CO stripping peak centered at ca. 0.76 V in the positive-going scan suggests that much of the adsorbed CO is still present on the catalyst surface. The quantitative evaluation of these data, following the procedure described above, shows that also in this case ca. 80% of the CO adlayer is still adsorbed on the Pt particles after 9 min exposure to the O_2-saturated sulfuric acid solution at 0.26 V, similar to the change in CO_{ad} coverage during reaction at 0.06 V (Figure 3). On the other hand, the amount of hydrogen peroxide produced in the H-upd region at E_{ad} = 0.26 V (Figure 4a−c) is only half of that generated after CO adsorption and reaction at 0.06 V (Figure 3a−c). A more detailed interpretation of these results will be given in the Discussion

3.2. Oxygen Reduction on Partly CO_{ad}-Covered Pt/Vulcan Catalyst Electrodes − Transient Chronoamperometric Measurements. The effect of the CO adlayer on the mechanism and kinetics of the ORR is much more directly evaluated in potentiostatic transient measurements, where the kinetic effects, the change in the overall ORR kinetics and in the contributions of the different reaction pathways with varying CO adlayer coverage, do not interfere with potential-dependent features such as H-upd or the onset of CO_{ad} electrooxidation in the "prewave" region.[33] Therefore, the current transients on both generator and

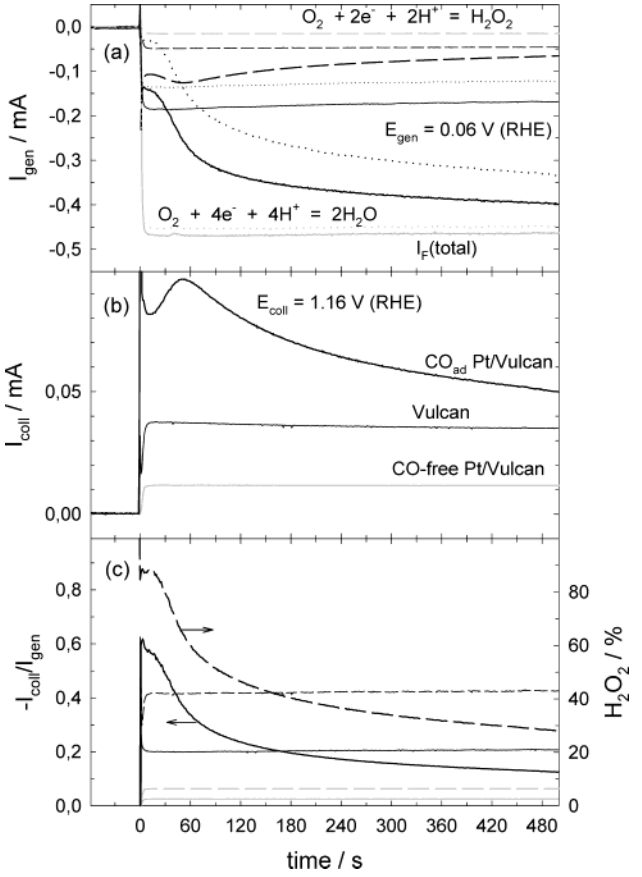

Figure 5. Simultaneously recorded current transients after starting O_2-saturated electrolyte flow over a CO_{ad}-blocked Pt/Vulcan catalyst (black thick lines), CO_{ad}-free Pt/Vulcan catalyst (gray lines) (Pt loading 28 μg/cm^2) or Vulcan carbon (black thin lines) at 0.06 V. (a) Faradaic current transients in the first compartment and (b) H_2O_2 oxidation currents on polycrystalline Pt (E = 1.16 V) in the second compartment of the dual thin-layer flow cell; (c) corresponding hydrogen peroxide yields. (Electrolyte flow rate ca. 4 μL/s, room temperature, assignment of the lines as in Figure 1.)

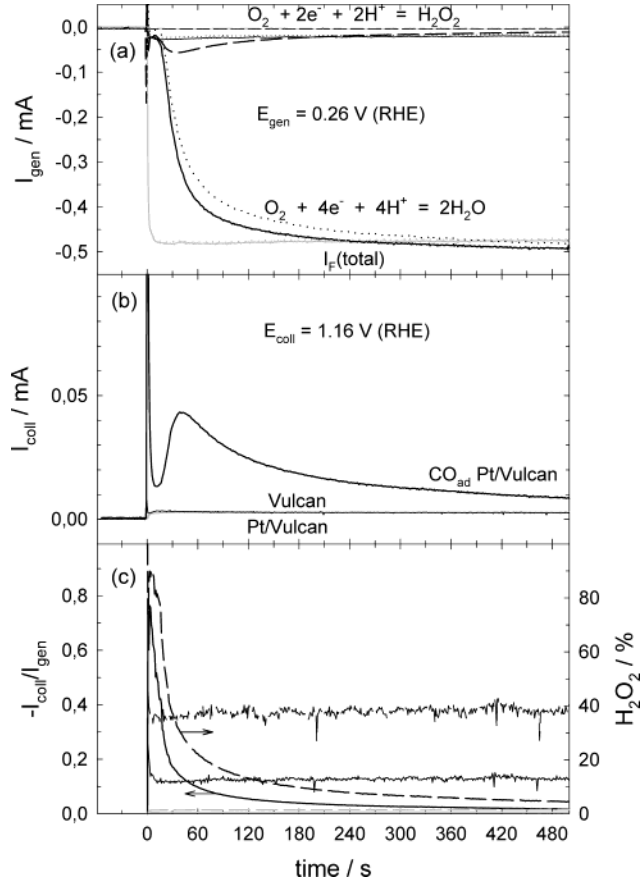

Figure 6. Simultaneously recorded current transients after starting O_2-saturated electrolyte flow over a CO_{ad}-blocked Pt/Vulcan catalyst (black thick lines), CO_{ad}-free Pt/Vulcan catalyst (gray lines) (Pt loading 28 μg/cm^2) or Vulcan carbon (black thin lines) at 0.26 V. (a) Faradaic current transients in the first compartment and (b) H_2O_2 oxidation currents on polycrystalline Pt (E = 1.16 V) in the second compartment of the dual thin-layer flow cell; (c) corresponding hydrogen peroxide yields. (Electrolyte flow rate ca. 4 μL/s, room temperature, assignment of the lines as in Figure 1.)

collector were recorded continuously during the combined ORR and chemical CO oxidation at 0.06 (Figure 5) and 0.26 V (Figure 6) on the CO_{ad}-covered Pt/Vulcan catalyst surface, respectively, for 8.5 min. Subsequently, the residual CO_{ad} was removed by electrochemical oxidation (CO stripping) to detect the CO_{ad} coverage (see Figures 3 and 4). For comparison, similar transients were recorded on a CO_{ad}-free Pt/Vulcan electrode (gray lines) and on a Vulcan support electrode (thin black lines) in O_2-saturated sulfuric acid solution (Figures 5 and 6). For all three electrodes, our previous DEMS measurements had shown a measurable consumption of O_2 during the reaction time[3]).

For reaction at 0.06 V (Figure 5, zero time corresponds to the onset of O_2-saturated electrolyte flow) on the Vulcan electrode and on the CO_{ad}-free Pt/Vulcan electrode, the O_2 reduction current almost instantaneously reaches its final value, which is equivalent to the mass transport limited current for the latter one and about 40% of that for the former one, (Figure 5a, solid gray line and solid thin black line). In contrast, on the CO_{ad}-blocked Pt/Vulcan electrode, the ORR current first exhibits a sharp spike and then returns to a value slightly lower than that on the Vulcan electrode. It then increases steadily with time, reaching about 80% of the ORR current on the CO-free Pt/Vulcan electrode after 8.5 min. The transient ORR behavior on the CO-blocked Pt/Vulcan electrode points to a significant effect of the slowly decreasing CO adlayer coverage on the ORR characteristics.

The proposition of a pronounced coverage adlayer effect on the formation of hydrogen peroxide is supported by the simultaneous measurements of hydrogen peroxide formation at the second electrode (Figure 5b, solid black line): The hydrogen peroxide oxidation current on the Pt collector shows, after an initial current spike, a continuous change on the CO_{ad}-blocked Pt/Vulcan electrode, first passing through a maximum value of ca. 0.1 mA ca. 50 s after starting the electrolyte flow and then dropping to ca. 0.06 mA after 8.5 min. The sharp collector current increase when starting the electrolyte flow is attributed to an experimental artifact, to oxidation of CO residues in the solution rather which were not completely removed during the brief flush of the flow cell with CO-free electrolyte, rather than to oxidation of hydrogen peroxide formed at the CO blocked Pt/Vulcan generator. According to the subsequent CO stripping data (Figure 3a, solid black line), the CO_{ad} coverage decreased to about 80% of its initial value during that time, reaching a final value of about 0.6 ML. In contrast, on both the CO_{ad}-free Pt/Vulcan electrode (Figure 5b, solid gray line) and on the Vulcan electrode (Figure 5b, thin black line), the hydrogen peroxide oxidation current and hence the hydrogen peroxide formation rate assume almost instantaneously their final, constant value, which on the latter is about 3-fold higher than on the CO_{ad}-free Pt/Vulcan electrode, at only 40% of the overall ORR current. These currents correspond to constant hydrogen peroxide yields of ca. 6% on the CO-free Pt/Vulcan electrode

(Figure 5c, gray dashed line) and about 42% on the Vulcan electrode (Figure 5c, thin black dashed line). The latter results agree very well with literature data.[17,34] The corresponding partial currents for O_2 reduction to hydrogen peroxide (dashed lines) and water (dotted lines) on carbon Vulcan (thin black lines), Pt/Vulcan (thick gray lines), and CO-blocked Pt/Vulcan (thick black lines), calculated according to eqs 1 and 2, are plotted in Figure 5a. On the fully CO_{ad}-covered Pt/Vulcan electrode, the hydrogen peroxide yield is initially constant for about 20 s, reaching ca. 90%, and then drops steadily to a value of ca. 30% after 8.5 min (Figure 5c, thick dashed line). As mentioned above, this loss in hydrogen peroxide yield goes along with a decay in the CO_{ad} coverage, from saturation (0.75 ML) to 80% of the saturation value (0.6 ML). As had been discussed before, similarly high hydrogen peroxide yields (up to 100%) where found during the ORR in RRDE measurements on several adsorbate covered Pt electrode surfaces (see section 3.1.1).

Analogous current transients for the ORR recorded at a constant electrode potential of 0.26 V are shown in Figure 6 (CO stripping of the CO adlayer remaining after these experiments is shown in Figure 4). In their general characteristics, these data closely resemble those obtained during reaction at 0.06 V (see above). On the CO_{ad}-blocked Pt/Vulcan surface, the total ORR current (Figure 6a, thick solid black line) also first increases almost instantaneously after having started the flow of O_2-saturated electrolyte. The value reached here, however, is only about -0.02 mA, which is only slightly more than 10% of that obtained at 0.06 V. It then decays steadily to the mass transport limited value of about 0.5 mA. Furthermore, despite the rather similar final values of the ORR current, the increase in ORR current is much faster at the higher potential. At 0.26 V, the ORR current reaches the same value in about 1 min as after 8.5 min at 0.06 V and attains the ORR value measured on the CO_{ad}-free Pt/Vulcan electrode at 0.26 V in ca. 4 min (Figures 6a and 5a, thick solid black and gray lines). Nevertheless, the amount of CO_{ad} remaining after the reaction, evaluated from the stripping peak after 9 min of CO-adlayer exposure to O_2-saturated solution at 0.26 V (Figure 4a, thick solid black line), is about the same as that after reaction at 0.06 V (Figure 3a, thick solid black line), i.e., about 80% of the saturated CO adlayer coverage, equivalent to about 0.6 ML.

These results explain in a simple way the different observations for the coverage of the remaining CO adlayer and hence for the rate for chemical CO_{ad} oxidation by chemical reaction with oxygen in our previous DEMS experiments,[3] where we found a much stronger decay of the CO adlayer coverage and hence faster CO_{ad} oxidation kinetics for reaction at 0.26 V than at 0.06 V, and in the present experiments, where the losses of the CO adlayer were similar at both potentials. The rates are indeed different for shorter reaction times, being significantly higher at 0.26 V than at 0.06 V. However, the reactions becomes very slow at longer reaction times and levels off the mass transport limited value, at a CO_{ad} coverage of about 0.6 ML. Apparently, at a critical CO_{ad} coverage of around 80% of the saturation coverage, there are enough free Pt sites available to reach the transport limited ORR rate, leaving very little O_2 for the chemical reaction with adsorbed CO (see the Discussion section). In the DEMS experiments, which were performed using a 2% O_2-in-Ar gas mixture, it takes much longer to reach this critical CO_{ad} coverage than in the present DDE-DTLFC experiments, where from experimental reasons we had to work with pure O_2. Hence, we had not waited long enough in the DEMS experiments in ref 3 to reach this CO critical coverage.

On the CO_{ad}-free Pt/Vulcan electrode (Figure 6a, thick solid gray line) and on the Pt-free Vulcan electrode (Figure 6a, thin solid black line) the initial and constant ORR currents at 0.26 V correspond to the mass transport limited value for the ORR and to the initial ORR current on the CO_{ad}-blocked Pt/Vulcan electrode, respectively. The latter result indicates that the initial ORR activity on the CO-blocked Pt/Vulcan electrode is determined by the ORR on the carbon support. Note that for reaction at 0.06 V (Figure 5a) the initial ORR activity on the CO_{ad}-blocked Pt/Vulcan electrode was slightly lower than that on the Pt-free Vulcan electrode.

The collector current measured for the ORR on the CO_{ad}-saturated Pt/Vulcan electrode shows a qualitatively similar transient behavior at 0.26 V as at 0.06 V. It immediately increases after the flow of O_2-saturated electrolyte was started, then decreases to a minimum after 10−15s, increases again and passes through the maximum after ca. 40s, and then slowly decays to finally reach a value of about 0.08 mA (Figure 6b, thick black line). On a quantitative scale, however, the hydrogen peroxide formation current is significantly higher at 0.06 V than at 0.26 V, by about a factor of 4, despite of the similar losses in CO_{ad} coverage in both cases (see the Discussion section).

For comparison, the ORR current on the CO_{ad}-free Pt/Vulcan electrode (Figure 6a, thick solid gray line) reaches its mass transport limited value within a few seconds after having started the flow of O_2-saturated electrolyte, similarly to observations at 0.06 V (Figure 5a, thick solid gray line). The hydrogen peroxide production at 0.26 V, however, reaches less than 20% of that at 0.06 V (Figures 6b and 5b, solid gray lines) and, correspondingly, also lower hydrogen peroxide yields (Figures 6c and 5c, dashed gray lines). Finally both the total ORR current and the hydrogen peroxide formation current on the Vulcan electrode (Figures 6a,b, thin black lines) are only about 10% of that at 0.06 V (Figure 5a,b thin black line), resulting in a similar hydrogen peroxide yield of about 40% (Figure 6c, thin dashed line). Compared to the reaction on the CO_{ad}-free Pt/Vulcan electrode at a similar reaction potential of 0.26 V the total ORR current reaches only about 10% (Figure 6a, thin solid black and solid gray lines) at similar hydrogen peroxide formation currents (Figure 6b, thin black and thick gray lines), in agreement with previous findings that carbon is a poor ORR catalyst compared to Pt.[10,34]

4 Discussion and Conclusions

The data presented above in combination with the DEMS data in ref 3 lead to the following conclusions on the kinetics and mechanism of the competing chemical CO_{ad} oxidation and the ORR on CO_{ad}-covered Pt/Vulcan catalysts.

1. At a fuel cell relevant reaction potential of 0.06 V, the chemical oxidation of CO_{ad} is rather slow. At a mass transport limited O_2 impingement of at least 10 ML per second, which is calculated from the mass transport limited ORR rate assuming a reaction probability of 1 on the CO_{ad}-free Pt/Vulcan catalyst under these conditions, it takes about 500 s to remove 20% of the adsorbed CO. For a CO_{ad} coverage independent reaction rate, we can calculate a reaction probability for chemical CO oxidation of at most 10^{-5} (5000 ML O_2 per 0.15 ML CO_{ad}) per impinging O_2 molecule from the above numbers.

2. The reaction rate for chemical CO oxidation depends strongly on the CO_{ad} coverage and on the potential, which is evidenced both by the Faradaic current, using the ORR rate as a measure for the CO_{ad} coverage, and by the CO_2 formation rate.[3,32] Under present reaction conditions, the limiting CO_{ad} coverage is about the same for both potentials investigated,

around 0.6 ML. At the same time, the O_2 consumption has reached the mass transport limited value. We therefore explain the observation of a limiting coverage by the combination of two effects, (i) a significant decrease in the probability for chemical CO oxidation (see point 4) and (ii) an increase in the O_2 consumption for the ORR, which leaves increasingly less oxygen for the competing CO oxidation.

3. Also the activity and selectivity of the ORR depend strongly on the CO_{ad} coverage. At both reaction potentials the initial H_2O_2 yield, on a fully CO_{ad}-blocked Pt/Vulcan catalyst, is between 80% and 90%, though at much lower rates at the higher potential. With increasing reaction time, and therefore decreasing CO_{ad} coverage, the H_2O_2 yield decreases steadily, reaching about 25% at the limiting CO_{ad} coverage of 0.6 ML, whereas the (negative) Faradaic current increases to the O_2 mass transport limited value.

4. The formation of a pronounced maximum in the rate for H_2O_2 formation after about 45−60 s under present reaction conditions, both at 0.06 and 0.26 V reaction potential, in combination with a steady increase in faradaic current and decrease in H_2O_2 yield with decreasing CO_{ad} coverage, points to a complex relation between the total ORR rate, described by the Faradaic current, and the H_2O_2 yield. Whereas in the first 60 s the increase in reactivity prevails, resulting in an increasing partial current for H_2O_2 formation, the decrease in H_2O_2 yield overcompensates this effect in the later stages. The maximum in H_2O_2 formation appears long before the mass transport limited O_2 consumption is reached, so that transport effects cannot be made responsible.

A mechanistic explanation of this phenomenon can be given when we include the observation of a similar maximum, after comparable reaction times, in the CO_2 formation rate.[3] The correlation between CO oxidation and H_2O_2 formation leads to the proposal that O_2 adsorption in small vacancies, most likely mono-vacancies, can result either in H_2O_2 formation *or* in reaction with a neighboring CO_{ad} (CO_2 formation) plus formation of H_2O. The probability for CO_{ad} oxidation, however, is much lower than that for H_2O_2 formation, pointing to a considerable reaction barrier for the latter process. Though we cannot rule out the reaction with two neighboring CO_{ad} molecules, it appears unlikely considering the very low probability for CO_{ad} oxidation, which even for a saturated CO adlayer is much less likely than reduction to H_2O. On the larger vacancies the ORR prevails, resulting in H_2O formation, while reaction of the reaction intermediate with CO_{ad}, at the perimeter of the vacancies, is highly improbable.

Reaction between a molecularly adsorbed peroxo species and CO_{ad} was in fact found in recent density functional calculations for CO oxidation on Pt(111) at high coverages as the lowest barrier reaction path.[35]

5. Comparison of the partial currents for H_2O_2 formation, $I_{H_2O_2}$, on the carbon Vulcan electrode and on the fully CO_{ad}-blocked Pt/Vulcan electrode shows a significantly lower rate for H_2O_2 formation on the latter electrode. Furthermore, the total O_2 consumption for the ORR on the carbon Vulcan electrode is also significantly higher than on the fully CO_{ad}-blocked Pt/Vulcan electrode. These results can only be explained by either inherent differences between the pure support material and the support of the Pt/Vulcan catalysts, or by a reduction in the number of active sites on the support material in the presence of the Pt nanoparticles.

6. Finally, we will briefly discuss some implications of this study for the air bleed operation of low-temperature polymer electrolyte fuel cells (PEFCs). Our DEMS[3] and DDE-DTLFC measurements imply that the oxidation of adsorbed CO by O_2 at fuel cell relevant anode potentials is a very slow process. Only 10^{-5}−10^{-4} of the consumed O_2 molecules are used for CO oxidation;[3] the vast majority is used in the ORR, with a very high yield for H_2O_2 formation, between 80 and 90% at saturation and still more than 25% at a CO_{ad} coverage of 80% of the saturation coverage. On the other hand, the loss of ca. 20% of the CO adlayer is sufficient to reach the diffusion-limited ORR current under present experimental conditions. Likewise, for the hydrogen oxidation reaction (HOR) on a CO blocked Pt/Vulcan electrode the loss of ca. 5% of the CO adlayer was found to be sufficient to reach the mass transport limited HOR rate under similar experimental conditions.[33]

On the basis of the effective CO sticking probability at a given CO adlayer coverage,[33] we can calculate the required minimum amount of O_2 in the feed to maintain a constant steady-state coverage of adsorbed CO. For 80% of the saturation coverage, the effective sticking probability of CO is around 0.3.[33] With a reaction probability of 3×10^{-5} for chemical CO oxidation and a CO contamination level of 50 ppm, this would require 15% O_2 in the feed gas to maintain this coverage. For 95% of the CO_{ad} saturation coverage, the required O_2 content would be somewhat lower because of the lower CO sticking coefficient (<0.1) and the higher reaction probability at the higher CO_{ad} coverage. Taking the H_2O_2 yield, however, the reduction in the amount of O_2 required would at least partly be offset by the much higher H_2O_2 yield at the higher CO_{ad} coverage, which is estimated to be between 60 and 80% compared about 25% at 80% of the saturation coverage. Hence, in both cases, about 3−4% of the feed would be turned into H_2O_2 under these conditions, which is not tolerable because of the possible degradation of the carbon support and the membrane.[5]

These numbers may vary significantly in the presence of H_2, at higher temperatures, and under the mass flow conditions present in an operating fuel cell. Nevertheless, it is instructive to visualize in a well-defined model setup the impact of the very low probability for chemical CO oxidation, by reaction with O_2, on a supported Pt catalyst. In a simplified picture, the "price" for increasing the CO tolerance of a fuel cell anode using the air-bleed method very likely is an enhanced long-term degradation of the MEA, i.e., of the catalyst layer, carbon support, and membrane due to the reasons discussed above.

Acknowledgment. We gratefully acknowledge financial support by the state of Baden-Württemberg, within the "Zukunftsoffensive Junge Generation", by the Federal Ministry of Education and Research (Grant 01SF0053) and by the Deutsche Forschungsgemeinschaft (Be 1201/8-4).

References and Notes

(1) Gottesfeld, S.; Pafford, J. *J. Electrochem. Soc.* **1988**, *135*, 2651.
(2) Gottesfeld, S.; Zawodzinski, T. A. In *Advances in Electrochemical Science and Engineering*; Alkire, R. C., Gerischer, H., Kolb, D. M., Tobias, C. W., Eds.; Wiley-VCH: Weinheim, Germany, 1997; Vol. 5.
(3) Jusys, Z.; Kaiser, J.; Behm, R. J. *J. Electroanal. Chem.* **2003**, *554*−*555*, 427.
(4) Zhang, J.; Thampan, T.; Datta, R. *J. Electrochem. Soc.* **2002**, *149*, A765−A772.
(5) Scherer, G. G. *Ber. Bunsen-Ges. Phys. Chem.* **1990**, *94*, 1008.
(6) Yu, J.; Yi, B.; Xing, D.; Liu, F.; Shao, Z.; Fu, Y.; Zhang, H. *Phys. Chem. Chem. Phys.* **2003**, *5*, 611.
(7) Jusys, Z.; Kaiser, J.; Behm, R. *J. Electrochim. Acta* **2004**, *49*, 1297.
(8) Frumkin, A. N.; Nekrasov, L.; Levich, V. G.; Ivanov, J. *J. Electroanal. Chem.* **1953**, *1*, 84.
(9) Damjanovic, A.; Genshaw, M. A.; Bockris, J. O. *J. Electrochem. Soc.* **1967**, *114*, 466.

(10) Tarasevich, M. R.; Sadkowski, A.; Yeager, E. In *Comprehensive Treatise in Electrochemistry*; Bockris, J. O. M., Conway, B. E., Yeager, E., Khan, S. U. M., White, R. E., Eds.; Plenum Press: New York, 1983.

(11) Markovic, N. M.; Gasteiger, H. A.; Ross, P. N. *J. Phys. Chem.* **1995**, *99*, 3411.

(12) Markovic, N. M.; Gasteiger, H. A.; Ross, P. N. *J. Phys. Chem.* **1996**, *100*, 6715.

(13) Markovic, N. M.; Ross, P. N., Jr. *Surf. Sci. Rep.* **2002**, *45*, 117.

(14) Watanabe, M. Saegusa, S.; Stonehart, P. *Chem. Lett.* **1988**, 1487.

(15) Mukerjee, S. *J. Appl. Electrochem.* **1989**, *20*, 537.

(16) Claude, E.; Addou, T.; Latour, J.-M.; Aldebert, P. *J. Appl. Electrochem.* **1998**, *28*, 57.

(17) Paulus, U. A.; Schmidt, T. J.; Gasteiger, H. A.; Behm, R. J. *J. Electrochem. Soc.* **2001**, *495*, 134.

(18) Schmidt, T. J.; Paulus, U. A.; Gasteiger, H. A.; Behm, R. J. *J. Electroanal. Chem.* **2001**, *508*, 41.

(19) Paulus, U. A.; Wokaun, A.; Scherer, G. G.; Schmidt, T. J.; Stamenkovic, V.; Radmilovic, V.; Markovic, N. M.; Ross, P. N., Jr. *J. Phys. Chem. B* **2002**, *106*, 4181.

(20) Maillard, F.; Martin, M.; Gloaguen, F.; Leger, J. M. *Electrochim. Acta* **2002**, *47*, 3431.

(21) Markovic, N. M.; Schmidt, T. J.; Stamenkovic, V.; Ross, P. N. *Fuel Cells* **2001**, *1*, 105.

(22) Paulus, U. A.; Schmidt, T. J.; Gasteiger, H. A. In *Handbook of Fuel Cells − Fundamentals, Technology and Applications*; Vielstich, W., Gasteiger, H. A., Lamm, A., Eds.; Wiley: New York, 2003; Vol. 2.

(23) Markovic, N. M.; Gasteiger, H. A.; Grgur, B. N.; Ross, P. N. *J. Electroanal. Chem.* **1999**, *467*, 157.

(24) Stamenkovic, V.; Markovic, N. M.; Ross, P. N. *J. Electroanal. Chem.* **2001**, *500*, 44.

(25) Mo, Y.; Scherson, D. A. *J. Electrochem. Soc.* **2003**, *150*, E39−E46.

(26) Markovic, N. M.; Lucas, C. A.; Gasteiger, H. A.; Ross, P. N. *Surf. Sci*. **1996**, *365*, 229.

(27) Abe, T.; Swain, G. M.; Sashikata, K.; Itaya, K. *J. Electroanal. Chem.* **1995**, *382*, 73.

(28) Stamenkovic, V.; Markovic, N. M. *Langmuir* **2001**, *17*, 2388.

(29) Jusys, Z.; Massong, H.; Baltruschat, H. *J. Electrochem. Soc.* **1999**, *146*, 1093.

(30) Schmidt, T. J.; Gasteiger, H. A.; Stäb, G. D.; Urban, P. M.; Kolb, D. M.; Behm, R. J. *J. Electrochem. Soc.* **1998**, *145*, 2354.

(31) Jusys, Z.; Kaiser, J.; Behm, R. J. *Langmuir* **2003**, *19*, 6759.

(32) Jusys, Z.; Behm, R. J. *Electrochim. Acta*, in press.

(33) Jusys, Z.; Kaiser, J.; Behm, R. *J. Phys. Chem. Chem. Phys.* **2001**, *3*, 4650.

(34) Kinoshita, K. *Electrochemical Oxygen Technology*; John Wiley & Sons: New York, 1992.

(35) Eichler, A.; Hafner, J. *Surf. Sci.* **1999**, *433*−*435*, 58.